GCA TECHNICAL REPORT NO. 65-1-N

51 Copies

# LOW MESOPAUSE TEMPERATURES OVER EGLIN TEST RANGE DEDUCED FROM DENSITY DATA

R. A. MINZNER G. O. SAUERMANN G. A. FAUCHER



GCA CORPORATION
Bedford, Massachusetts

CONTRACT NO. NASw-976

PREPARED FOR

NATIONAL AERONAUTICS AND SPACE ADMINISTRATION

WASHINGTON, D. C.

JANUARY 1965

GCA Technical Report 65-1-N

# LOW MESOPAUSE TEMPERATURES OVER EGLIN TEST RANGE DEDUCED FROM DENSITY DATA


R. A. Minzner G. O. Sauermann

G. A. Faucher*


January 1965


Contract No. NASw-976



GCA CORPORATION
Bedford, Massachusetts

*Air Force Cambridge Research Laboratories



Prepared for

NATIONAL AERONAUTICS AND SPACE ADMINISTRATION
Washington, D. C.

ABSTRACT

19769

Unusually low values of temperature (about 156 $\pm$ 16°K) have been found to exist in the region of 100 km altitude over Eglin Gulf Test Range in Florida (30° 24' N, 86° 43' W) at 2315 hours GMT on December 7, 1961. These low temperatures have been determined from 50 density-altitude data points over the altitude range of 97.8 km to 132.2 km, without the use of any independent temperature information. The basic density data and their associated uncertainties were deduced from measurements of drag accelerations on a falling sphere of 2.74 meters diameter [1].* The data are shown graphically in Figure 10 of that paper and numerical values of density $\rho$ and its uncertainties $\delta\rho$ are summarized in Table 2 of that same paper. The uncertainties in temperature which are dependent upon $\delta\rho$ have been calculated. From the extent of the temperature uncertainty, it is apparent that the temperature-altitude profile is well bounded for altitudes below 110 km, especially for the lower two kilometers of the profile, and these low mesopause temperatures are therefore indeed significant.

AUTHOR

*Numbers in [ ] throughout text indicate reference numbers.

LOW MESOPAUSE TEMPERATURES OVER EGLIN TEST RANGE
DEDUCED FROM DENSITY DATA

The method for obtaining the temperature $T_r$ at any altitude $Z_r$ involves the downward integration of atmospheric mass density $\rho$ with respect to Z from $Z_a$ to $Z_r$ where $Z_a$ is the greatest altitude of usable data. The basic form of the equation for extracting the temperature information from the density-altitude data is a well-known relationship [2,3,4] based on the hydrostatic equation and the equation of state:

$$T_r = \frac{\rho_a}{\rho_r} T_a + \frac{\overline{M}}{R\rho_r} \int_{Z_r}^{Z_a} (g\rho)\, dZ \tag{1}$$

where $\rho_a$ and $\rho_r$ are densities at altitudes $Z_a$ and $Z_r$, respectively,

$T_a$ is the temperature at $Z_a$,

$\overline{M}$ is the mean molecular weight of the gas (considered to be constant),

R is the universal gas constant, and

g is the acceleration of gravity.

At first glance it would appear that the presence of $T_a$ in Equation (1) would prevent the evaluation of $T_r$ since no information about $T_a$ is available. It is seen, however, that when the density-altitude gradient is negative, as it is in the atmosphere, the term $(\rho_a/\rho_r)T_a$ becomes negligibly small as altitude $Z_r$ is taken sufficiently below $Z_a$, while the integral term approaches the full value of $T_r$. The highest 15 to 20 km of mass-density data are consumed in essentially eliminating the $T_a$ term, and the more reliable values of $T_r$ are determined only for lower altitudes; i.e., below 110 km for the data at hand.

In dealing with real mass-density data of a multigas atmosphere where the acceleration of gravity and the mean molecular weight are variables with respect to altitude, it is convenient to introduce two transformations. First, the two variables T and $\overline{M}$ are combined into a single new variable $T_M$ (molecular scale temperature) through the relationship $T_M \equiv (T/\overline{M})M_o$ where $M_o$ is the sea-level value of $\overline{M}$ [4,5,6,7,8]. Second, the two variables g and Z are combined into a single new variable h (geopotential) through the relationship $G\cdot dh = g\cdot dZ$ where G is a constant numerically equal to the sea-level value of g [5,6,7,9]. In addition, the existence of the data in the form of discrete density-altitude points makes it desirable to introduce the trapezoidal rule for numerical integration. Together, these transformations lead to

$$(T_M)_r = \frac{\rho_a}{\rho_r} (T_M)_a + \frac{GM_o}{R\rho_r} \left[ \rho_a \left( \frac{h_a - h_{a+1}}{2} \right) + \rho_r \left( \frac{h_{r-1} - h_r}{2} \right) + \sum_{j=a+1}^{r-1} \rho_j \left( \frac{h_{j-1} - h_{j+1}}{2} \right) \right]. \tag{2}$$

In this expression the density-data points are considered to be numbered consecutively such that the numbers increase downward from the point at $Z_a$ which is identically point "a" or point No. 1.

From this equation, $T_M$ is determined as a function of h in geopotential meters (m'), but, by a reverse transformation, the values of h are independently related to appropriate values of Z, so that $T_M$ is finally available as a function of geometric altitude Z.

In Figure 1, a series of five solid-line profiles of $T_M$ versus Z computed from the data by means of Equation (2) are compared with $T_M$ of the U. S. Standard Atmosphere [8]. These five curves are representative of an infinite number of profiles which might be computed from the data, each differing solely by virtue of the assumed value of $(T_M)_a$ at 132.2 km, the upper end of the useful available density data. Each of the series of five values of $(T_M)_a$ employed, differs by 200°K from the preceding value, with the range extending from 173.7°K to 973.7°K. The $T_M$ profiles are seen to converge with decreasing altitude.

Since any expected true value of $T_M$ at 132.2 km should be well within the extremes of the five values of $(T_M)_a$ presented, the true $T_M$-versus-Z profile should also always lie between the extreme curves even at low altitudes where these curves are separated by 10° or less. Thus, for altitudes below 110 km, the value of $T_M$, without consideration for density uncertainty, appears to be bounded within narrow limits; 40° at 110 km and 3° at 98 km.

A rigorous error analysis based on the Gaussian method indicates that $(\delta T_M)_r$, the uncertainty in $(T_M)_r$, is given by

$$(\delta T_M)_r = \left[ \left( \frac{u}{\rho_r} \right)^2 + \left( \frac{\rho_a}{\rho_r} (\delta T_M)_a \right)^2 \right]^{\frac{1}{2}} \tag{3}$$

where $(\delta T_M)_a$ is the uncertainty in $(T_M)_a$ and

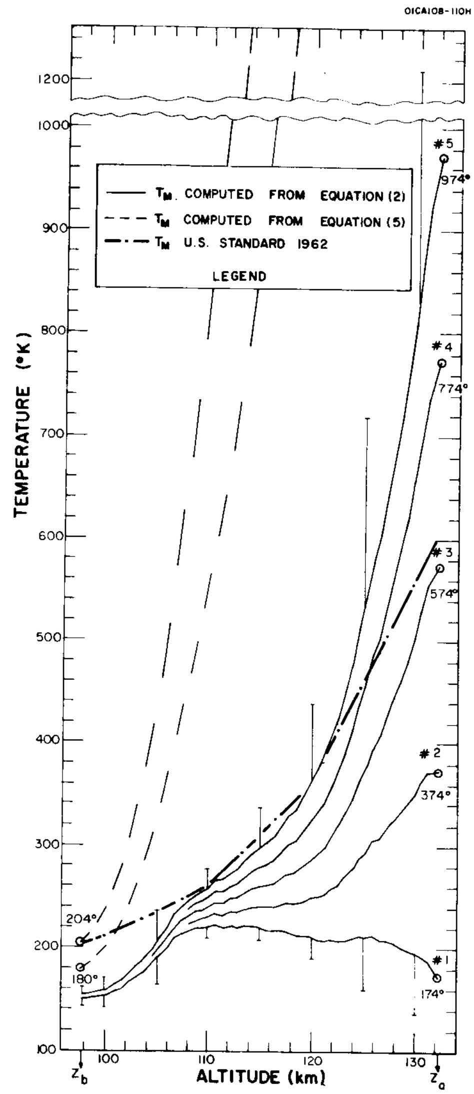


Figure 1. Temperature versus altitude.

$$\left(\frac{u}{\rho_r}\right)^2 = \left[(T_M)_a + \frac{GM_o}{R}\left(\frac{h_a - h_{a+1}}{2}\right)\right]^2\left(\frac{\delta\rho_a}{\rho_r}\right)^2 + \left[(T_M)_r - \frac{GM_o}{R}\left(\frac{h_{r-1} - h_r}{2}\right)\right]^2\left(\frac{\delta\rho_r}{\rho_r}\right)^2$$

$$+\left(\frac{GM_o}{R}\right)^2 \sum_{j=a+1}^{r-1}\left(\frac{\delta\rho_j}{\rho_r}\right)^2\left(\frac{h_{j-1} - h_{j+1}}{2}\right)^2 \quad . \qquad (4)$$

In this expression, $\delta\rho_a$, $\delta\rho_j$ and $\delta\rho_r$ are the uncertainties in $\rho_a$, $\rho_j$ and $\rho_r$, respectively.

As in the case of Equation (1), the expression for the temperature uncertainty, Equation (3), also may not be evaluated for altitudes near $Z_a$, due to lack of information, in this instance, concerning $(\delta T_M)_a$. The ratio $(\rho_a/\rho_r)$, however, again serves essentially to eliminate the need for the unknown quantity when $Z_r$ is sufficiently below $Z_a$. This is illustrated graphically on the basis of the previous assumption that $(T_M)_a$ is within the range 173.7° to 973.7° such that $(\delta T_M)_a$ must be less than 800° which is the separation of the extreme curves at 132.2 km. Under these conditions, $(\rho_a/\rho_r)(\delta T_M)_a$ must be less than the separation of these two curves at any altitude $Z_r$. Therefore, it is apparent from the graph that at $Z_r$ = 100 km, $(\rho_a/\rho_r)(\delta T_M)_a$ is considerably less than 5°. Under these conditions, $(\delta T_M)_r$ is approximately equal to $\pm$ $(u/\rho_r)$ alone.

For any of the assumed values of $(T_M)_a$ it is possible to compute values of $\pm(u/\rho_r)$ versus $Z_r$ over the entire altitude range of the data in order to evaluate the influence of density uncertainty alone on the five computed profiles. The positive half of this uncertainty component $\pm(u/\rho_r)$ for Curve No. 5 is indicated by the upward directed flags on Curve No. 5, while the negative half of this uncertainty component for Curve No. 1 is indicated by the downward directed flags along this curve. For altitudes of 115 km and below, the values of $\pm(u/\rho_r)$ appear to be reasonably small even for Curve No. 5. Thus, considering both the convergence of the $T_M$-versus-Z profiles and the uncertainties $\pm(u/\rho_r)$, $T_M$ is well bounded for altitudes below 110 km.

It is also possible to rewrite Equation (2) so that the reference level is at $Z_b$, the lowest altitude of available data, and the temperature at altitude $Z_s$ is obtained by the upward integration of density from $Z_b$ to $Z_s$. Thus,

$$(T_M)_s = \frac{\rho_b}{\rho_s}(T_M)_b - \frac{GM_o}{R\rho_s}\left[\rho_b\left(\frac{h_{b+1} - h_b}{2}\right) + \rho_s\left(\frac{h_s - h_{s-1}}{2}\right) + \sum_{j=b+1}^{s-1}\rho_j\left(\frac{h_{j+1} - h_{j-1}}{2}\right)\right] \quad (5)$$

where $\rho_b$ and $\rho_s$ are densities at altitudes $Z_b$ and $Z_s$,
$(T_M)_b$ is an unknown value of $T_M$ at altitude $Z_b$, and
$(T_M)_s$ is the computed temperature at altitude $Z_s$.

The subscript s implies upward integration from $Z_b$ to $Z_s$ to obtain $(T_M)_s$, and for this equation, the data points are numbered consecutively increasing upward from the point at $Z_b$ which is identically point b or point No. 1.

Again an infinite number of profiles of $T_M$ versus Z are possible, each associated with one of an infinite number of possible choices of the unknown $(T_M)_b$. In this instance, however, the ratio $(\rho_b/\rho_s)$ is always greater than 1 and the members of any pair of curves of $T_M$ versus Z for different values of $(T_M)_b$ diverge with increasing altitude by the amount of $\Delta T_b(\rho_b/\rho_s)$. Thus, any uncertainty in $(T_M)_b$ is also magnified by that ratio. Furthermore, both the ratio term and the integral term become very large as Z increases; hence the uncertainty in their difference, and also in $(T_M)_s$, increases beyond any useful limits. When the assumed value of $(T_M)_b$ is 180° or 204.0° (the latter being equal to that of the U. S. Standard Atmosphere for $Z_b$), Equation (5) yields values of $(T_M)_s$ represented by the dashed lines which diverge rapidly from the U. S. Standard values to unrealistically high values as Z increases above 110 km. When $(T_M)_b$ is taken to be successively 151.4664, 152.2602, 153.8478, and 154.6416 degrees, Equation (5) develops identically the five solid-line curves computed by Equation (2). The initial selection of a reference temperature of 153.05 $\pm$ 1.59°, however, is most unlikely; and for that part of the atmosphere where the mean molecular weight is high; i.e., where $N_2$ and $O_2$ are the predominant gases, it is apparent that Equation (5) is useless. For high altitudes, however, where He or $H_2$ dominates the atmosphere [10,11,12] such that the mean molecular weight is small and the logarithm of the density-altitude gradient is proportionately reduced, one may show that it is better to develop the temperature-altitude profile upward from a moderately well-known $(T_M)_b$ by means of Equation (5) than to work downward from a completely unknown $(T_M)_a$ by means of Equation (2).

The above analysis shows the value of $T_M$ at 100 km over Eglin Gulf Test Range to be 157 $\pm$ 13° while at 97.8 km $T_M$ is 152 $\pm$ 9°. From the shape of the curve this latter value appears to be essentially the mesopause minimum although no data exist for lower altitudes during this flight. From the previously cited definition it is apparent that $T_M$ is greater than T by a factor $M_o/M$, the value of which varies with altitude essentially as shown in Table 1. This table was prepared using the values of M from the U. S. Standard Atmosphere [8] and hence these values should be reasonably reliable, at least for altitudes Z < 130 km. The related difference in degrees between $T_M$ and T for the median curve (No. 3) of Figure 1 is also given in this table. It is apparent that the difference between the plotted values of $T_M$ and the related values of T is small compared with the uncertainties in $T_M$ at all altitudes involved in this study. Thus, while the graph is strictly a plot of $T_M$, it adequately represents kinetic temperature T for all practical purposes, particularly for the altitudes below 110 km.

This mesopause temperature of 152 degrees Kelvin is only 75 percent of the standard-atmosphere value and is low compared with the mean wintertime mesopause value for that latitude as indicated by Court et al. [13]. Instances of similarly low mesopause temperatures have been observed on several other occasions: (1) over Wallops Island, 38° north latitude, on 20 June 1963 [14]; (2) over the Marshall Island, 10° south latitude, on 23 January 1964 [14]; (3) over Fort Churchill, 58° north latitude, on 21 July 1957 [15]; and (4) over Russia during the summer, year and latitude unspecified [16]. Apparently, such low mesopause temperatures are not too unusual in tropical or semitropical regions at various seasons of the year, in contrast with arctic regions where low mesopause temperatures are generally observed only during the summer months.

TABLE 1

VALUES OF $M_o/M$ AND $(T_M - T)$ VERSUS ALTITUDE Z

| Z<br>km | $M_o/M$<br>dimensionless | $T_M - T$<br>degrees K |
|---|---|---|
| 90 | 1.000 | 0.00 |
| 100 | 1.003 | 0.47 |
| 110 | 1.014 | 3.6 |
| 120 | 1.032 | 9.2 |
| 130 | 1.050 | 25.2 |

## SUMMARY AND CONCLUSIONS

1. In the absence of independent temperature information, a single profile of mass density versus altitude yields a $T_M$-versus-altitude profile, which does not depart drastically from a T-versus-altitude profile for altitudes below 130 km.

2. The altitude range of reliable $T_M$ values extends from about 15 to 20 km below the greatest altitude of reliable density data down to the lowest altitude for which data are obtained.

3. A temperature T of 152 $\pm$ 10°K which is low in comparison with average mesopause temperature values is reported for 98 km altitude over Eglin Gulf Test Range, Florida.

4. This value is similar to other low values of the mesopause temperature observed on at least four different occasions and locations.

## REFERENCES


1. Faucher, G. A., Procunier, R. W., and Sherman, F. S., "Upper-Atmosphere Density Obtained from Measurements of Drag on a Falling Sphere," J. Geophys. Res. 68, 3437-3450 (1963).

2. Elterman, L., "A Series of Stratospheric Temperature Profiles Obtained with the Searchlight Technique," J. Geophys. Res. 58, 519-530 (1953).

3. Newell, H. E., Jr., "High Altitude Rocket Research," Academic Press, Inc., New York, 1953 (p.112).

4. Champion, K. S. W. and Minzner, R. A., "Revision of United States Standard Atmosphere 90 to 700 km," Rev. of Geophys. 1, 57-84 (1963).

5. Minzner, R. A. and Ripley, W. S., "The ARDC Model Atmosphere 1956," Air Force Surveys in Geophysics No. 86, ARCRC TN-56-204 (1956).

6. Minzner, R. A., Ripley, W. S., and Condron, T. F., "U. S. Extension of the ICAO Standard Atmosphere," Washington, D.C. (1958).

7. Minzner, R. A., Champion, K. S. W., and Pond, H. L., "The ARDC Model Atmosphere 1959," Air Force Surveys in Geophysics No. 115, AFCRC TR-59-267 (1959).

8. "U. S. Standard Atmosphere," National Aeronautics and Space Administration, U. S. Air Force, and U. S. Weather Bureau, Government Printing Office, Washington, D.C. (1962).

9. Harrison, L. P., "Relation between Geopotential and Geometric Height," Smithsonian Meteorological Tables, R. S. List, Ed., 6th Edit., 217-218, Washington, D.C. (1951).

10. Miller, L. E., "Molecular Weight of Air at High Altitudes," J. Geophys. Res. 62, 351-356 (1957).

11. Sauermann, G. O. and Herzog, R. F. K., "Helium in the Earth's Atmosphere," GCA Tech. Rpt. No. 61-6-N (1961).

12. Spencer, N. W., Newton, G. P., Reber, C. A., Brace, L. H., and Horowitz, R., "New Knowledge of the Earth's Atmosphere from the Aeronomy Satellite (Explorer XVII)," X-651-64-114, Goddard Space Flight Center, Greenbelt, Maryland (1964).

13. Court, A., Kantor, A. J., and Cole, A. E., "Supplementary Atmospheres," AFCRL-62-889 (September 1962).

14. Peterson, J. W., private connumication (1964).

15. Stroud, W. G., Nordberg, W., Bandeen, W. R., Bartman, F. L., and Titus, P., "Rocket-Grenade Measurements of Temperatures and Winds in the Mesosphere over Churchill, Canada," J. Geophys. Res. 65, 2307-2323 (1960).

16. Mikhnevich, V. V. and Khvostikov, I. A., "Study of the Upper Layers of the Atmosphere," Akademiia Nau SSSR, Leningrad, Izvestiia, Seriia Geofizicheskiia No. 11, 1393-1409 (1957).